THE

PHYSICAL REVIEW

Decay of Tl²¹⁰ to States of Pb²¹⁰†

P. WEINZIERL, E. UJLAKI, AND G. PREINREICH

*Institute for Physics, Reactor Center, Seibersdorf, SGAE, Seibersdorf, Austria, and
First Physics Institute, University Vienna, Vienna, Austria*

AND

G. EDER

Institute for Theoretical Physics, University of Vienna, Vienna, Austria

(Received 11 October 1963)

The decay of Tl²¹⁰ sources was investigated by means of scintillation and semiconductor spectrometers. $\beta-\gamma$, $\gamma-\gamma$, and γ-sum-coincidence measurements were carried out. The β spectrum (from shell-model considerations presumably a first-forbidden transition) was decomposed into three components of 2.34 ± 0.10, 1.87 ± 0.10, and 1.32 ± 0.10 MeV. Twenty-four γ lines were found decomposing the NaI(Tl) scintillation spectrum; six of them showed measurable conversion lines in the semiconductor spectrometer and their transition type could be inferred. Measurements of the delay of different parts of the γ spectrum with respect to the β rays revealed the existence of at least three states of measurable half-life, 1.7 ± 0.1, 1.1 ± 0.1, and 0.6 ± 0.1 nsec, the latter arising from the second excited state of 1.09 MeV. Calculations of the Pb²¹⁰ levels were carried out, using a zero-range approximation for the interaction between the two extra neutrons and compared with the experimental level scheme.

I. INTRODUCTION

THE level schemes of most nuclei in the neighborhood of the double closed-shell nucleus Pb²⁰⁸ have been carefully investigated already and a considerably good agreement with theoretical calculations has been achieved in some cases.[1-3] The theoretical approach starts from experimentally given single-particle levels of one extra nucleon (or hole) in the field of the core; the levels of a nucleus containing two or more extra nucleons (or holes) are then calculated, basing their interaction on different assumptions.[4-6]

The experimental evidence for the levels of the nucleus Pb²¹⁰ (containing two extra neutrons in addition to the Pb²⁰⁸ core) was insufficient up to now for such con-

siderations. Mayer-Kuckuck's investigation[7] of the Tl²¹⁰ decay revealed a threefold γ cascade in Pb²¹⁰ (0.783, 0.297, and 2.36 MeV), which, together with a 1.96-MeV β transition, yielded the correct decay energy.[8] Earlier work of one of the present authors[9] showed the complex character of this decay, while experimental data were not sufficient for the construction of the decay scheme.

The great experimental difficulty in the investigation of the Tl²¹⁰ decay arises from the fact that, according to the very low branching ratio in the Bi²¹⁴ (RaC) decay[10,11] $[(2-4)\times10^{-4}]$, only quantities of a few microcuries of Tl²¹⁰ can be prepared even starting with 0.5–1 Ci radon as source for the active deposit of Bi²¹⁴. Together with the 1.3-min half-life of Tl²¹⁰, this limits severely the applicability of experimental methods and also the statistical accuracy of results, especially in coincidence measurements.

[1] D. E. Alburger and M. H. L. Pryce, Phys. Rev. **95**, 1482 (1954).
[2] D. Stromminger, F. S. Stephens, Jr., and J. O. Rasmussen, Phys. Rev. **103**, 748 (1956).
[3] R. W. Hoff and J. M. Hollander, Phys. Rev. **109**, 447 (1958).
[4] N. Newby, Jr. and E. J. Konopinski, Phys. Rev. **115**, 435 (1959).
[5] M. H. L. Pryce, Proc. Roy. Soc. (London) **A65**, 773 (1952).
[6] W. True and K. Ford, Phys. Rev. **109**, 1675 (1958).
[7] Th. Mayer-Kuckuck, Z. Naturforsch. **11a**, 627 (1956).
[8] K. Way, N. B. Gove, C. L. McGinnis, and R. Nakasima, *Energy Levels of Nuclei A=21 to A=212, Landolt-Börnstein I* (Springer-Verlag, Berlin, 1961).
[9] P. Weinzierl, Sitzber. Öst. Akad. Wiss. IIa **166**, 139 (1957).
[10] W. B. Lewis and B. V. Bowden, Proc. Roy. Soc. (London) **A145**, 235 (1937).
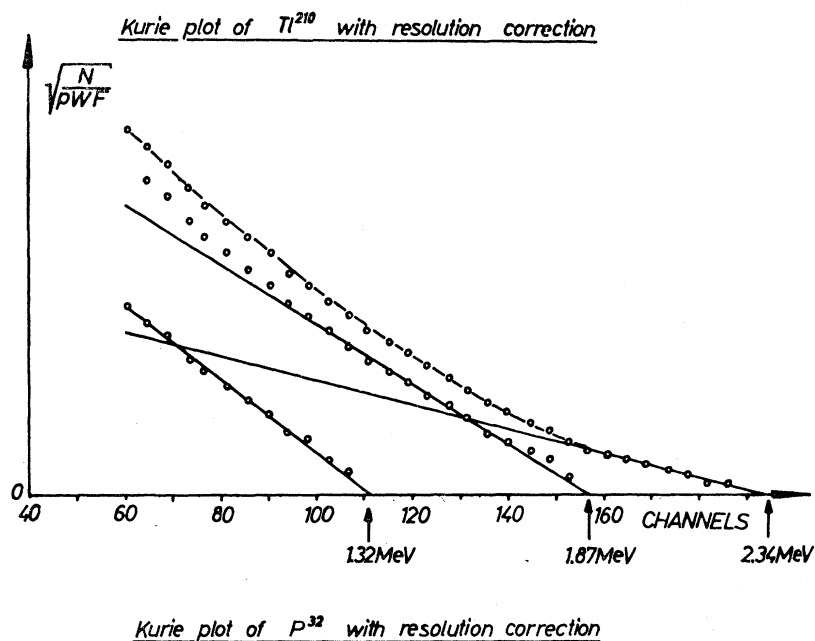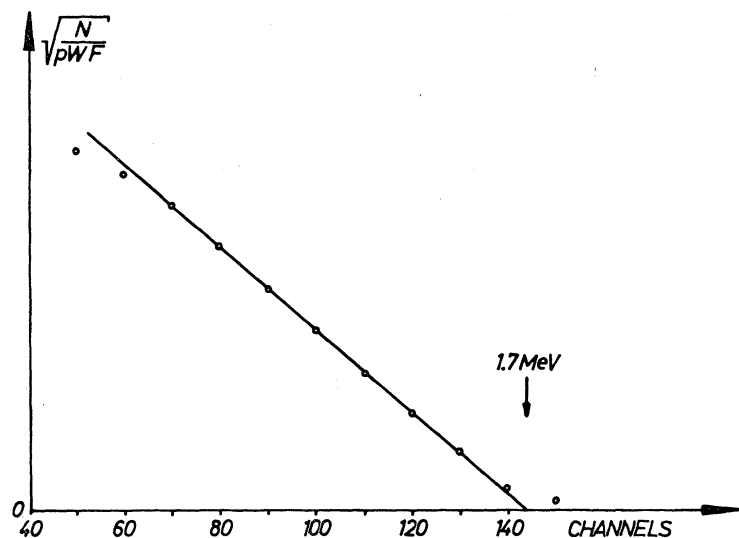[11] W. J. Chang, Phys. Rev. **74**, 1195 (1948).

Kurie plot of Tl²¹⁰ with resolution correction

$\sqrt{\dfrac{N}{pWF}}$

40   60   80   100   120   140   160 CHANNELS

1.32MeV   1.87MeV   2.34MeV

FIG. 1. Kurie plot and decomposition of the Tl²¹⁰ β spectrum (the P³² β spectrum is measured under identical conditions and included for comparison).

Kurie plot of P³² with resolution correction

$\sqrt{\dfrac{N}{pWF}}$

1.7MeV

40   60   80   100   120   140 CHANNELS

II. EXPERIMENTAL

A. Preparation of Tl²¹⁰ Sources

The purity of the radon, used for preparing the active deposit of $Pb^{214} - Bi^{214}$ (RaB+C) is very important for the quality of the Tl²¹⁰ (RaC″) sources, produced by the α-recoil method from this deposit. As radon source a solution containing 1.5 g radium was available.[12] The prepurification of the radon consisted of flashing the admixed hydrogen and oxygen gas and removing the main content of water vapor and CO_2 by KOH. The final

purification was based on a differential cooling method[13]: The radon was trapped in a liquid air bath after passing through a cooling loop of about −110°C, where impurities were retained. The purified radon was then brought in contact with a highly polished stainless steel plate, on which the active deposit was collected, by applying an electric field. The activated sample was heated to about 350°C in vacuum for about 10 min[14] in order to remove absorbed radon from the surface. After this the sample was stored for 60 min allowing for the decay of the α-emitting Po^{218} (RaA) by a factor of 10⁶. Then the preparation of Tl²¹⁰ sources was started by means of the
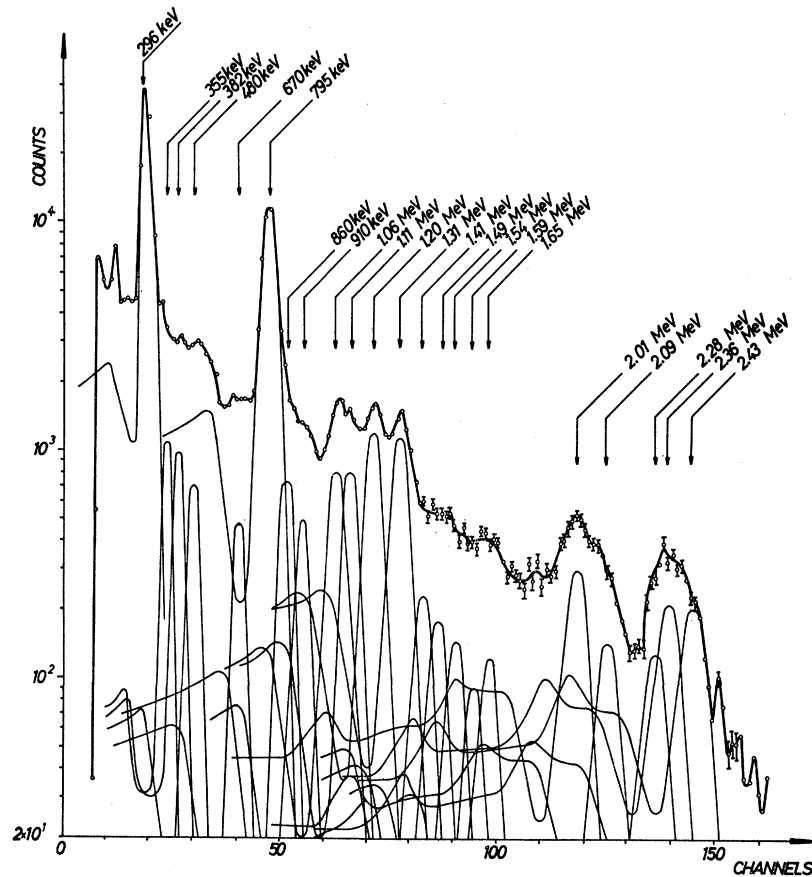
FIG. 2. Spectrum of Tl²¹⁰ γ rays in a 3-in.×3-in. NaI(Tl) crystal with spectrum analysis.

α-recoil method. Tin foils were used for the collection of Tl²¹⁰ activity in order to avoid α-induced reactions in the foil. The Tl²¹⁰ sources (activity of the order of 1 μCi) were of satisfactory purity, containing only a few percent of Pb²¹⁴—Bi²¹⁴ contamination. Sources were always used for measurements during 1 min only in order to keep the contribution of this long-lived contamination as small as possible.

B. β Spectrum

Earlier measurements by means of the absorption method[15] and by means of a scintillation spectrometer[7] led to an end-point energy of 1.8 and 1.96±0.1 MeV, respectively. Mayer-Kuckuck[7] found a simple β spectrum (1.96 MeV, logft=5.1) coincident with the main γ lines. Daniel[16] set an upper limit of 0.5% for higher energy components (>3 MeV) in the β spectrum. Kogan and Rusinoff[17] and Bensch[18] deduced a very faint (∼10⁻⁵/decay) low-energy β component from their observation of delayed neutrons.

[15] S. Devons and G. J. Neary, Proc. Cambridge Phil. Soc. **33**, 154 (1937).
[16] H. Daniel, Z. Naturforsch. **12a**, 194 (1957).
[17] A. Kogan and L. I. Rusinov, Zh. Eksperim. i Teor. Fiz. **32**, 432 (1957) [English transl.: Soviet Phys.—JETP **5**, 365 (1957)].
[18] F. Bensch, Phys. Letters (to be published).

The continuous β spectrum was investigated by means of an anthracene scintillation spectrometer with multichannel analyzer. The anthracene crystal was 1 cm thick and covered by a 2-mg/cm² Al foil. The registered β spectrum of Tl²¹⁰ was corrected experimentally with respect to the Tl²¹⁰ γ rays and with respect to the β and γ rays from the Pb²¹⁴—Bi²¹⁴ contamination of the sources. A resolution correction was applied to the Tl²¹⁰ β spectrum, using the half-width of the Cs¹³⁷ K-conversion line, measured under identical conditions, and a $E^{-1/2}$ dependence of the resolution on β energy.

Figure 1 shows the Kurie plot of the obtained β spectrum of Tl²¹⁰. The β spectrum of P³² measured and corrected in the same way is included for comparison. The corrected Tl²¹⁰ spectrum shows a definitely stronger curvature of the Kurie plot than the P³² spectrum. As a first-forbidden transition seems very likely (according to the ft values and to shell-model considerations outlined below), this curved Kurie plot suggests a complex β decay and a decomposition was attempted. Although this seems hardly possible in a unique way for the given accuracy of the measurement, the β components shown on Fig. 1 match well the γ cascades observed (see Sec. E). The estimated intensities of the β components
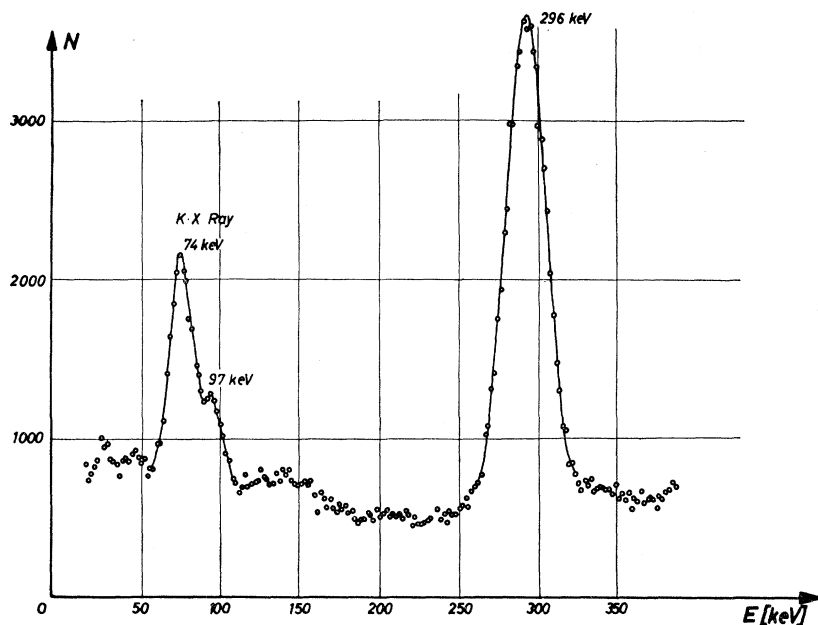
FIG. 3. Low-energy γ spectrum of Tl[210] in a $1\frac{1}{2}$-in.$\times$2-in. NaI(Tl) crystal.

are:

$$2.34\pm0.10 \text{ MeV}\cdots19\%,$$

$$1.87\pm0.10 \text{ MeV}\cdots56\%,$$

$$1.32\pm0.10 \text{ MeV}\cdots25\%.$$

A consideration of spins and parities of the nucleonic states before and after the β decay leads to a rather clear prediction for the type of β transition of Tl[210]: The decaying Tl[210] ground state contains (in addition to the Pb[208] core) one proton hole in $3s_{1/2}$ level, one unpaired $2g_{9/2}$ neutron and a neutron pair. Their combination leads probably to 5^+ or 4^+ for the Tl[210] ground state. Apart from the pair of extra neutrons the state after the β decay (transforming one neutron into a proton) presumably corresponds to the state of Pb[208] immediately after the Tl[208] decay containing an excitation of the Pb[208] core, one proton hole ($3s_{1/2}$), and one extra proton in a higher level ($2h_{9/2}$ or $2f_{7/2}$). These excited core states have negative parity; as the possible configurations of the two extra neutrons in Pb[210] have positive parity, they do not change the over-all negative parity of the final state. Therefore, a β transition from a state of positive parity to a state of negative parity can be expected. From the $\log ft$ values of the Tl[210] decay—$\log ft$ (2.36 MeV)$=6.2$, $\log ft$ (1.87 MeV)$=5.3$, $\log ft$ (1.32 MeV)$=5.2$—we conclude that a first-forbidden β decay is very likely.

C. γ Spectrum and Conversion Electrons

Due to the low source intensities available, the method of analyzing complex γ spectra in single NaI(Tl) crystals by successive subtracting of standard

spectra shapes as introduced by Lazar[19] and Heath[20] seemed the only possibility of obtaining more information. Figure 2 shows the γ spectrum registered in a 3-in.$\times$3-in. NaI(Tl) crystal and the analysis obtained by this subtraction method. A separate measurement of the low-energy γ spectrum was carried out with a $1\frac{1}{2}$-in.$\times$2-in. NaI(Tl) crystal on a RCA 7326 photomultiplier with high photocathode efficiency (Fig. 3). The complex low-energy peak on Fig. 3 can also be resolved considering the detailed structure[21] of the K x-ray peak. A 97-keV γ ray is then seen clearly. The existence of an additional weak line around 85 keV is possible but uncertain. Table I gives the values for the γ energies and intensities obtained. The intensities are quoted relative to an intensity of 100 for the strongest γ line at 795 keV.

A semiconductor detector was used for conversion line analysis (RCA type-A 400). This detector—cooled by dry ice—gave a resolution of 1.6% for the Cs[137] K-conversion line.

A special amplifier system (ORTEC, type 101–201) was used incorporating an adjustable bias before the last amplifier stages. Figure 4 shows the electron spectra obtained for two different bias settings, corrected already for the Pb[214]—Bi[214] contamination. The spectrum with 3-V bias shows definite conversion lines at 208-, 268-, 281-, and 294-keV electron energy and a weak line at about 720 keV. The efficiency of the semiconductor spectrometer was determined by simultaneous recording of the γ spectrum of the sources in a 3-in.$\times$3-in. NaI(Tl)

[19] N. H. Lazar, IRE Trans. Nucl. Sci. NS5, 138 (1958).
[20] R. L. Heath, Atomic Energy Commission Research and Development Report IDO-16408 (unpublished).
[21] A. H. Wapstra, G. J. Nijgh, and R. van Lieshout, Nuclear Spectroscopy Tables (North-Holland Publishing Company, Amsterdam, 1959).

FIG. 4. Conversion electron spectra of Tl²¹⁰ in a semiconductor spectrometer with two different bias settings in the amplifier.
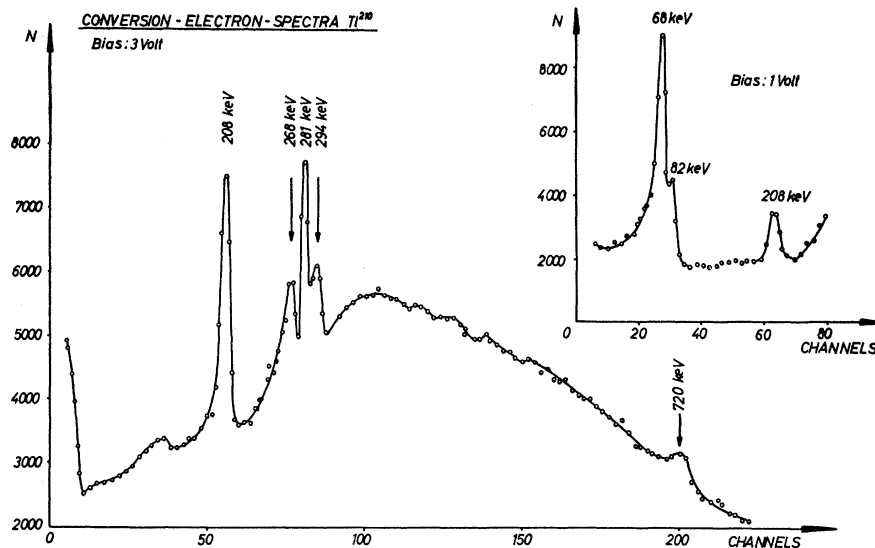
crystal with known efficiency and comparison to the conversion electron spectrum of Tl²⁰⁸ under identical conditions. So the intensities quoted refer also to an intensity of 100 for the 795-keV γ ray. The 208- and 281-keV conversion lines with intensities of 5.8 and 2.7, respectively, are easily ascribed to the 296-keV transition (intensity 80) yielding conversion factors $\alpha_K=0.072$ and $\alpha_L=0.034$. From the tables of Rose,[22] one obtains $\alpha_2(K)=0.067$

TABLE I. Tl²¹⁰ γ transitions.

Energy (MeV)	γ intensity[a]	K line[a]	L line[a]	Multi-polarity
K x ray	20±4			
0.083±0.03[b]	(2)[c]		25 ±5	(E2)[c]
0.097±0.03	4±2	(11)[c]	4 ±2	M1+E2
0.296±0.003	80±10	5.8±1.0	2.7±0.5	E2
0.356±0.01[b]	4±2	1.1±0.2		M1
0.382±0.01	3±2	0.9±0.2		M1
0.48 ±0.02	2±1			
0.67 ±0.02	2±1			
0.795±0.003	100	1.0±0.3		E2
0.86 ±0.03	7±2			
0.91 ±0.03	3±2			
1.06 ±0.02	12±5			
1.11 ±0.02	7±2			
1.21 ±0.02	17±4			
1.31 ±0.02	21±5			
1.41 ±0.02	5±2			
1.49 ±0.02	2±1			
1.54 ±0.03	2±1			
1.59 ±0.03	2±1			
1.65 ±0.03	2±1			
2.01 ±0.03	7±2			
2.09 ±0.03	5±2			
2.28 ±0.03	3±2			
2.36 ±0.03	8±3			
2.43 ±0.03	9±3			

[a] Relative to intensity 100 for the 795-keV γ line; according to the results of Sec. D. This agrees within 10% with an intensity quoted in percent/decay.
[b] Energy determined by conversion electron measurement.
[c] Not directly measured, value deduced from indirect evidence.

[22] M. E. Rose, *Internal Conversion Coefficients* (North-Holland Publishing Company, Amsterdam, 1958).

and $\alpha_2(L)=0.039$ for an E2 transition interpolated for this energy. The conversion lines at 268 keV (intensity 1.1) and 294 keV (intensity 0.9) are thought to be K lines of transitions at 356 and 382 keV. An E1 or E2 classification of these lines would call for a much higher γ intensity at these energies than compatible with the results of the γ-spectrum decomposition. E2 would also require corresponding L-conversion lines of noticeable intensities in the spectrum, which are not visible. Therefore, M1 seems the proper classification for the 356- and 382-keV transition. The intensity (~1) of the weak line near 720 keV is compatible with an E2 transition at 795 keV.

A marked rise at the low-energy end of the spectrum with 3-V bias setting stimulated the measurement with lower bias (1 V). Although the resolution is poorer, a prominent and complex low-energy peak is found around 68-keV electron energy. The interpretation of these conversion lines can be attempted referring to the low-energy γ spectrum shown on Fig. 3. The badly resolved electron line at 82 keV is interpreted as L line of the 97-keV transition. The K conversion of this transition is too low energetic to be visible in the spectrum, but the corresponding K x-ray intensity accounts for the otherwise unexplained high intensity of the K x-ray peak. For a M1 transition at 97 keV, $\beta_1(K)=9.0$ and $\beta_1(L)=1.2$; for an E2 transition, $\alpha_2(K)=0.58$, $\alpha_2(L)=4.5$.[22] A mixed M1+E2 transition could account for the required contribution to the K x-ray peak and for the intensity of the L-conversion line at 82 keV. The strong electron line around 68 keV is interpreted as L-conversion line of a 83-keV transition, which lies below the K-binding energy in lead. For an E2 transition the intensity of the 68-keV line can be explained assuming a corresponding weak 83-keV γ line hidden in the unresolved low-energy γ peak of Fig. 3. As no positive evidence for a γ ray at 83 keV exists, the possibility of
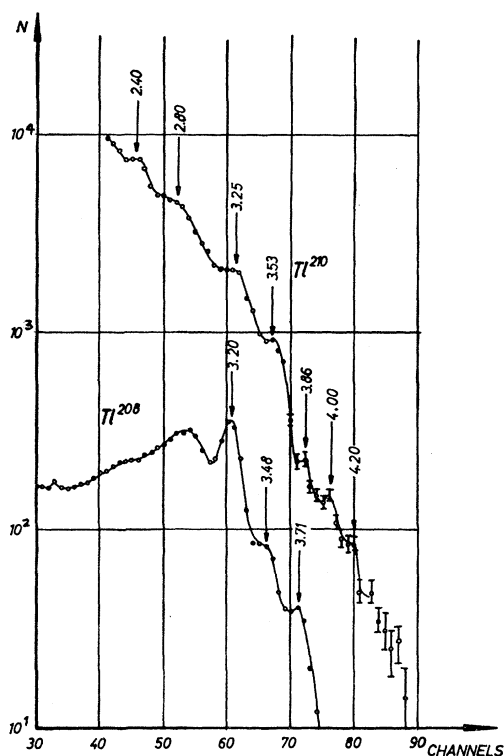
FIG. 5. γ-sum coincidence spectra of Tl²¹⁰ and Tl²⁰⁸.

a L-converted $0^+ \rightarrow 0^+$ transition must also be considered. From arguments discussed in Sec. G this interpretation was finally rejected.

The results of the conversion electron measurements are included in Table I, quoting intensities of measured conversion lines and multipolarities deduced from these.

It should be noted that taking the high conversion into account, one has to assume two low-energy transitions of $M1+E2$ and $E2$ type at 97 and 83 keV, with approximate total intensities of 19 and 27, respectively. This result is important for the interpretation of lifetime measurements reported in Sec. F.

D. Decay Energy Considerations and Search for Long-Lived Isomeric States in Pb²¹⁰

The decay energy of Tl²¹⁰ can be easily deduced from the decay energies of the Bi²¹⁴—Po²¹⁴—Pb²¹⁰ branch of the Bi²¹⁴ decay and the α energy of this nucleus. One obtains a value of 5.4 MeV.[8] Although the γ cascades observed and the β components add up satisfactorily to this decay energy, the situation is not quite as favorable if the γ intensities are also taken into account. In an earlier investigation[9] the uncompletely resolved γ spectrum led to the conclusion that the γ energy emitted per Tl²¹⁰ decay was much less than required. If one assumes that the 795-keV γ ray is emitted with an intensity of 100% per decay, one can deduce from the values quoted in Table I and the results of Sec. B the sum of β and γ energies released per decay. One obtains

4.7 MeV per decay. Although the discrepancy is less than the one reported earlier and the errors introduced by the method of γ-spectrum analysis are difficult to estimate, it stimulated a search for long-lived isomeric states reached in Tl²¹⁰ decay. This possibility is further supported by the fact that from the $(1i_{11/2}, 2g_{9/2})$ configuration of the two extra neutrons in Pb²¹⁰ spin states up to 10^+ are to be expected between 1.5–2 MeV (see theoretical part). Together with the known 9^- state in[23] Bi²¹⁰ the situation would be quite favorable for a β decay between these states.

Actually all attempts to detect long-lived isomeric transitions were unsuccessful and only lower limits for their intensities can be given.

(1) No α branch from an excited state of Pb²¹⁰ exists with an intensity higher than 0.5%, unless the α energy coincides within 1% with the 5.99-MeV line of Po²¹⁸ present as contamination. (The same statement holds for an α branch from the Tl²¹⁰ ground state. Dzhelepov and Peker[24] quote an uncertain α branch with 0.04% intensity.)

(2) The study of the decay curve of Tl²¹⁰ samples prepared with exposure times up to 60 min in the recoil apparatus showed three β half-lives: the 1.30±0.03 min half-life of Tl²¹⁰, the effective half-life of the Pb²¹⁴—Bi²¹⁴ decontamination of 22 min, and a very weak long-lived activity. The intensity of the latter is compatible with the Pb²¹⁰ contamination occurring during the α-recoil process.

(3) No γ-emitting isomer was found in Tl²¹⁰ decay with an intensity higher than 1% and a half-life between 3 and 300 min.

It has been suggested[25] that the discrepancy in the γ energy emitted per decay could be removed, if one assumes that two γ transitions occur in the decay with energies close to 795 keV and contribute both to the observed highest intensity peak in the scintillation spectrum. Their added intensities could easily exceed 100% per decay. As all other γ intensities are measured relative to the 795-keV peak, this would obviously yield a higher value of γ energy/decay. Therefore, a measurement of the intensity of the 795-keV line per Tl²¹⁰ β decay was carried out in a 4πβ-γ coincidence arrangement. By this method the absolute source strength is determined and the γ spectrum can be recorded at the same time on a multichannel analyzer. If the efficiency of the γ channel is calibrated, the γ intensity/β decay results immediately. We obtained $(103\pm10)\%$ γ_{795}/decay.

Therefore, all the intensities given in Table I agree with the intensity in percent/decay within approximately 10% accuracy.

[23] L. I. Rusinov, Zh. Eksperim. i Teor. Fiz. **40**, 1007 (1961) [English transl.: Soviet Phys.—JETP **13**, 707 (1961)].

[24] B. S. Dzelepov and L. K. Peker, *Decay Schemes of Radioactive Nuclei* (Pergamon Press Inc., New York, 1961).
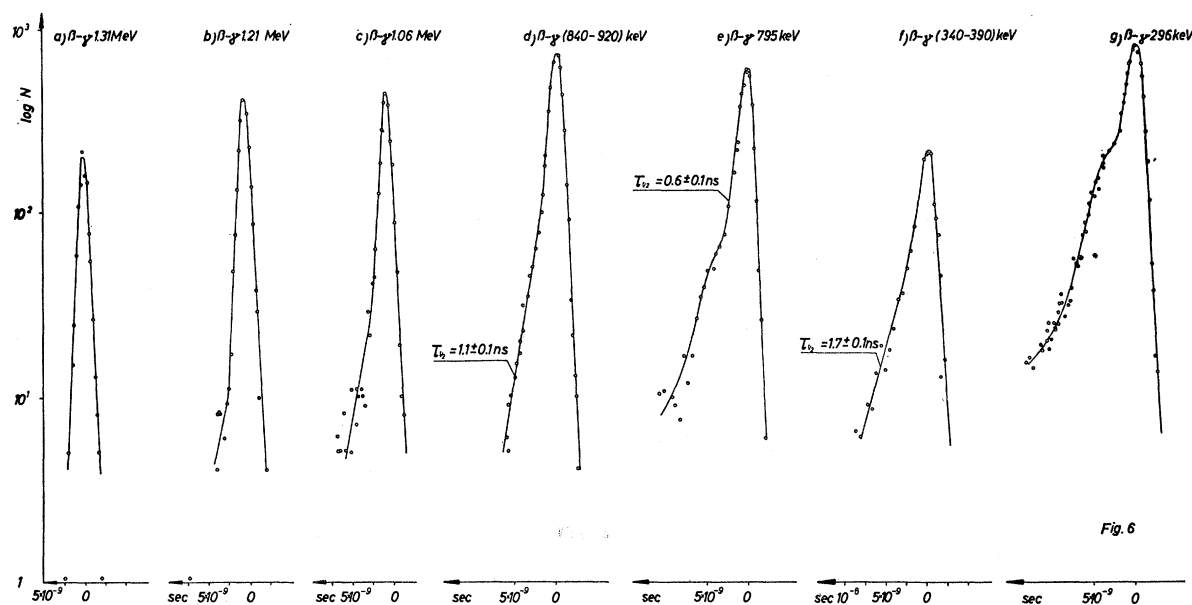
[25] H. Daniel (private communication).

FIG. 6. Delayed β-γ coincidence measurements with Tl^{210}; the γ-energy range selected is indicated on the figure, β energies were not discriminated.

E. Prompt Coincidence Measurements

γ-γ coincidence measurements were carried out using 3-in.$\times$3-in. and 4-in.$\times$4-in. NaI(Tl) crystals. The sample was located in the hole of an anti-Compton shield of 2-cm lead inserted between the crystals. Coincidence spectra were measured with the selecting single-channel analyzer set on the 296 keV and on the 795-keV line and with settings on the low-energy and high-energy part of the broad maximum around 2.4 MeV and on the energy interval between 335 and 385 keV. A quantitative evaluation of coincidence probabilities[26] was not possible due to the poor statistics of these measurements. Only the following conclusions could be drawn:

(1) The 795-keV γ ray is in coincidence with all other γ lines.

(2) The 296-keV γ ray is not in coincidence with the lines at 1.06 MeV, 2.01 MeV and either the 2.28- or the 2.36-MeV lines.

(3) The 2.43-MeV γ ray is in coincidence with the γ rays at 296, 480, and 795 keV.

(4) The 2.36-MeV γ ray is in coincidence with the 794- and the 296-keV line.

(5) The 356- and/or the 382-keV γ ray is in coincidence with the 1.41-, 1.49-, 1.54-, and 1.65-MeV γ line.

Further attempts have been made to apply the sum coincidence method.[27] It turned out that the sum spectrum of the coincident γ lines showed some interesting features, while the analysis of the lines contributing to a certain sum peak was not successful due to the high number of badly separated sum levels and the poor statistics.

[26] E. Ujlaki, Acta Phys. Austriaca **16**, 289 (1963).
[27] J. Hoogenboom, Nucl. Instr. **3**, 57 (1958).

Figure 5 shows the sum spectrum of Tl^{210} and—for comparison—also the sum spectrum of Tl^{208}. Sum peaks of high intensity occur around 3.53 and 3.25 MeV. They are broad and possibly complex and are interpreted as γ cascades including and not including, respectively, the 296-keV transition. A γ cascade with 2.4-MeV sum energy is shown clearly. The existence of sum levels as high as 3.86 and 4.00 MeV (eventually even one at 4.20 MeV) supports the idea of a complex β transition (Sec. B).

F. Delayed β-γ Coincidence Measurements

In a β-γ-coincidence experiment with a resolving time of 5.10^{-8} sec all γ rays above 200 keV appeared as prompt. This means that the lifetime of all levels reached in Tl^{210} decay are considerably shorter than the resolving time used (or much longer than 1 min, the counting time of each Tl^{210} source; but this is excluded by the results of Sec. D).

Delayed β-γ-coincidence measurements were carried out using a 6BN6 time-to-pulse-height converter stage. The betas were detected in a 2-mm plastic scintillator (NE102) without energy discrimination, the γ rays in a 1$\frac{1}{2}$-in.$\times$2-in. NaI(Tl) crystal; the γ energy was selected by a single-channel analyzer. 56 AVP photomultipliers were used in a conventional fast-slow arrangement.

Figure 6 shows the results obtained for different settings of the γ-energy channel. The proper operation of the equipment was ensured by the comparison with prompt curves obtained under identical conditions. Two of these delay curves (e and g) show an interesting shape, which—as far as we know—has not been observed before. The bumps in the slope of a delay curve can be interpreted assuming, e.g., in addition to a

prompt contribution, a multiple (at least twofold) delay of the γ ray selected with respect to the betas. An analysis of such complex delay curves leads to the following:

(1) The observed delay curve of a transition with respect to a timing event (e.g., a β decay) is given by the sum $N_0 + N_1(\lambda_1) + N_2(\lambda_1,\lambda_2) + N_3(\lambda_1,\lambda_2,\lambda_3)$ where N_0 is a prompt contribution and N_i are the delay curves corresponding to single delay (λ_1), double delays (λ_1,λ_2), etc. A bump in the slope of the experimental over-all delay curve can occur if the contrubution of at least one of the inner terms of the above sum is lacking or weak relative to the others.

(2) The slope of a delay curve $N_i(\lambda_1,\lambda_2\cdots\lambda_n)$ reaches finally the value of the longest lifetime $\tau_m = 1/\lambda_m$ involved.

(3) The final slope and the shift of the centroid of N_i with respect to the centroid of the prompt curve yields at least an estimate on the number and magnitude of decay constants λ_i. (The bump in the slope of the observed delay curve is much more pronounced if several short lifetimes are involved as compared to the case, when only one lifetime corresponding roughly to the sum of the other lifetimes occurs.)

Curve a in Fig. 6 is perfectly prompt. Curves b and c show a slight admixture of a lifetime in the 1-nsec region.

Curves e and g show pronounced similarity of their complex delay characteristics. It can therefore be safely assumed that these two strong γ transitions feed each other. The upper part of both delay curves shows a delay of 0.6 ± 0.1 nsec, determined by the centroid shift method. According to the level order fixed in Sec. G, the 296-keV transition feeds the 795-keV level. The 0.6-nsec lifetime is therefore ascribed to the 296-keV transition. (The Weisskopf estimate[21] gives 4 nsec for an $E2$ transition of this energy.) The bump indicates that the 1.09-MeV level is partially fed by successively delayed transitions. The decreasing slope of the delay curves shows that also a lifetime of several nanoseconds must be among the preceding transitions.

Curve 6 d is measured with a γ energy interval between 840 and 920 keV. The strong prompt contribution is probably due to Compton events accepted at this energy setting. The 860- and/or the 910-keV transition (or a preceding transition) must be responsible for the shown delay (final slope 1.1 ± 0.1 nsec).

Figure 6 f is obtained with an γ energy setting between 340 and 390 keV. In addition to a prompt contribution a single delay of 1.7 ± 0.10 nsec is shown clearly. The 355- and/or the 382-keV transition (or a preceding transition) must exhibit this characteristic.

G. Construction of Decay Scheme

The 795 keV with an intensity of $(104\pm10)\%$ per β decay, exhibiting the most complex delay curve structure with respect to the β ray is most likely to be the ground-state transition. The K-conversion factor of $(1.0\pm0.3)10^{-2}$ agrees with the expectation of a $E2$ transition from a first excited 2^+ state.

The high total intensity of the 296-keV transition and the similarity between the delay characteristics of the 296- and 795-keV transition made it rather certain that this transition feeds the 795-keV 2^+ level. The $E2$ classification of this level being certain from the conversion electron measurement (and in reasonable agreement with the 0.6 ± 0.1 nsec lifetime of the 1.09-MeV level) requires 4^+ or 0^+ for the second exited state. The second possibility is not compatible with the fact, that no transition from higher states go to the 0^+ ground state directly, while a high intensity feeds the 1.09-MeV level.

The possibility of a L-converted $E0$ transition at 83 keV is open from the γ spectrum and conversion line analysis; but the Pb^{210} ground state being 0^+ and the intensities of this L-conversion line and the 795-keV transition differing by a factor of 4, the only possibility for a $0^+ \rightarrow 0^+$ transition would be through a γ cascade parallel to the 795-keV transition leading to a first excited 0^+ state of 83 keV. But this disagrees (1) with the absolute intensity of the 795-keV transition, and (2) with the fact that all γ lines appear as coincident with this γ line. Therefore, the $E0$ classification for the 83-keV transition was discarded. The only other interpretation for this transition, taking the certainly high conversion factor $(\gtrsim 10)$ and a lifetime small compared to 5×10^{-8} sec into account, is $E2$. The comparison with the theoretical level scheme gives the main argument for placing this transition directly above the 1.09-MeV 4^+ level: while here a low-energy $E2$ transition is to be expected between the 6^+ and 4^+ level of the $(2g_{9/2})^2$ neutron configuration, it seems very unlikely to find such an intensive $E2$ transition in the upper part of the level scheme, where levels of adjacent spin values are accessible. As experimental evidence the delay curves (Fig. 6 e,g) are quoted: the 296-keV as well as the 795-keV transition show in the lower part of the delay curve the admixture of a lifetime of several nanoseconds. This lifetime is probably due to the preceding 83-keV $E2$ transition for which the Weisskopf estimate yields $\sim10^{-7}$ sec.[21] If, however, this transition would occur in the upper part of the scheme, other delay curves would also have to show this characteristic admixture.

The complete decay scheme suggested is shown in Fig. 7. The γ-γ coincidence and γ-sum results, the β-spectrum decomposition and the delay curves (Fig.6 d,f) are used for its construction. As a $M1$ transition of 356 keV would yield according to Weisskopf's formula a half-life of 10^{-12} sec, we ascribed the measured half-life of 1.7 nsec to a preceding 97-keV transition of $M1+E2$ characteristic.

Transitions and levels which are only energetically fitted between levels obtained from other evidence, are shown as dotted lines on Fig. 7. Transition energies are indicated in accordance with Table I. Discrepancies of
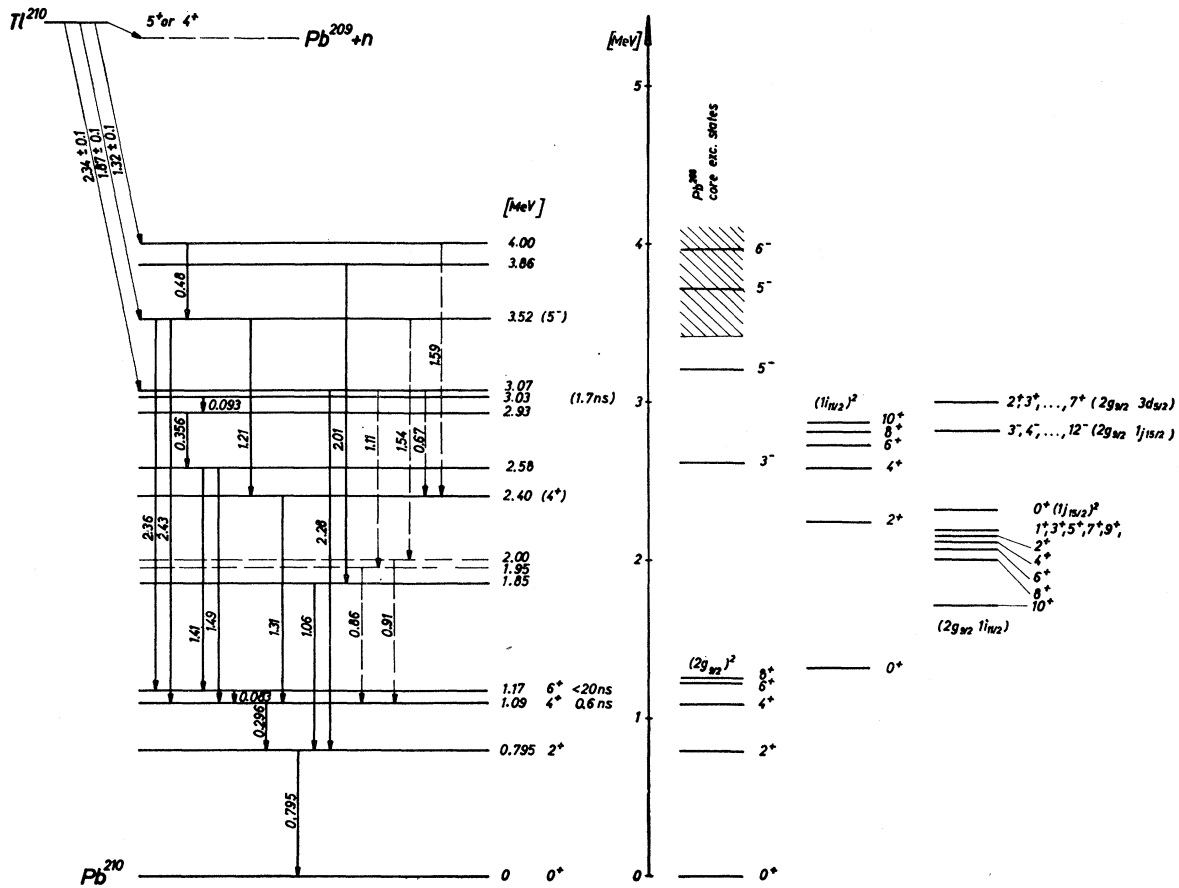
FIG. 7. Decay scheme of Tl²¹⁰; on the right side the level structure in Pb²¹⁰ is given as obtained by a calculation with δ forces for the two extra neutrons.

energy sums yielding the level energies were admitted within ±0.01 MeV.

III. THEORETICAL LEVEL STRUCTURE OF Pb²¹⁰

As already outlined in Sec. B, the Pb²¹⁰ nucleus is likely to be formed in Tl²¹⁰ decay in a proton configuration $(3s_{1/2}^{-1}, 1h_{9/2})$ or $(3s_{1/2}^{-1}, 2f_{7/2})$ with angular momentum $J = 4^-, 5^-,$ or 3^-. These levels are due to excitation of the Pb²⁰⁸ core and must be also expected after the Tl²⁰⁸ β decay. Actually the following levels are reached directly in Tl²⁰⁸ decay[8] (energy in keV, spin and parity)

2614(3⁻), 3198(5⁻), 3475(4⁻), 3708(5⁻), 3691(6⁻).

These levels combined with the configurations of the two extra neutrons give the excitations of Pb²¹⁰. The two neutrons outside of the Pb²⁰⁸ core occupy the single-particle levels which are known from the excitations of Pb²⁰⁹, where only one neutron is outside the closed neutron shell with $N = 126$. The low-lying states of Pb²⁰⁹ are[28,29] (energy in keV, configuration):

$0(2g_{9/2})$, $780(1i_{11/2})$, $1410(1j_{15/2})$, $1570(3d_{5/2})$, ···.

[28] H. Pollak, Bull. Akad. Roy. Belg. 47, 1035 (1961).
[29] P. Mukherjee and B. L. Cohen, Phys. Rev. 127, 1284 (1962).

Two neutrons arranged in these levels lead to the following states, if their interaction energy is neglected (energy in keV, configuration, spin and parity):

0	$(2g_{9/2})^2$	0⁺, 2⁺, 4⁺, ···, 8⁺
780	$2g_{9/2} 1i_{11/2}$	1⁺, 2⁺, 3⁺, ···, 10⁺
1410	$2g_{9/2} 1j_{15/2}$	3⁻, 4⁻, 5⁻, ···, 12⁻
1560	$(1i_{11/2})$	0⁺, 2⁺, 4⁺, ···, 10⁺
1570	$2g_{9/2} 3d_{5/2}$	2⁺, 3⁺, 4⁺, ···, 7⁺.

The splitting of these levels can be calculated for zero-range forces by the methods of de Shalit[30] and Newby and Konopinski.[5] We use oscillator wave functions in order to determine the Slater integrals. For zero-range forces, the interaction between two neutrons is effective in the singlet spin state only.

Therefore, we have only one parameter $k = (V_0/r_0^3)$ for the strength of the interaction. The radius r_0 determines the range of the oscillator wave functions: $u_{nl}(r \propto \exp(-r^2/2r_0^2))$. But we expect that a zero-range force overestimates the interaction energy of the two neutrons in states with $J = 0^+$. Thus, we assume that the interaction energy for $J = 0^+$ is only a fraction α of the energy derived on the basis of zero-range forces. The two parameters k and α are chosen in such a way

[30] A. de Shalit, Phys. Rev. 91, 1479 (1953).

that the three lowest levels of Pb²¹⁰ with the neutron configuration $(2g_{9/2})^2$ are in agreement with the experimental levels $0(0^+)$, $795(2^+)$, $1090(4^+)$. This yields $k=73.767$ keV and $\alpha=0.5565$. The pairing energy for the two neutrons in the ground state of Pb²¹⁰ becomes 1409 keV and agrees within the limits of error with the known binding energies of the Pb isotopes[31] (1355 ± 85) keV. These two parameters are used for the calculation of interaction energies in all configurations, as no experimental evidence exists for the identification of levels from higher configurations With the Pb²⁰⁸ core in its ground state, the following levels result up to 3 MeV (energy in keV, spin and parity):

$0(0^+)$, $795(2^+)$, $1090(4^+)$, $1220(6^+)$, $1252(8^+)$, $1316(0^+)$, $1715(10^+)$, $1988(8^+)$, $2067(6^+)$, $2115(4^+)$, $2152(2^+)$, $2189(1^+,3^+,5^+,7^+,9^+)$, $2242(2^+)$, $2312(0^+)$, $2581(4^+)$, $2724(6^+)$, $2811(8^+)$, $2819(3^-,4^-,5^-,\cdots,12^-)$, $2880(10^+)$, $2979(2^+,3^+,4^+,\cdots7^+)$.

If the Pb²⁰⁸ core is excited, the energy levels are disturbed by the interaction between the Pb²⁰⁸ core and the two extra neutrons. It is difficult, however, to estimate this interaction. If one neglects this interaction, the combination of the excited core states with the two-neutron configurations leads to the following states (energy in keV, spin and parity):

$2614(3^-)$, $2198(5^-)$, $3409(1^-,2^-,3^-,\cdots,5^-)$, $3475(4^-)$, $3704(1^-,2^-,3^-,\cdots,7^-)$, $3708(5^-)$, $3834(3^-,4^-,5^-,\cdots,9^-)$, $3866(5^-,6^-,7^-,\cdots,11^-)$, $3930(3^-)$, $3961(6^-)$, $3993(3^-,4^-,5^-,\cdots,7^-)$, $4270(2^-,3^-,4^-,\cdots,6^-)$, $4288(1^-,2^-,3^-,\cdots,9^-)\cdots$.

On Fig. 7 the groups of levels resulting from the different two-neutron configurations are shown separately up to

---
[31] L. A. König, J. H. E. Mattauch, and A. H. Wapstra, Nucl. Phys. **31**, 18 (1962).

an energy of 3 MeV. The pure core-excited states as obtained from Tl²⁰⁸ decay are indicated, while the level region resulting from a combination of core excitations and two-neutron states is shown as a shaded area above 3409 keV.

IV. DISCUSSION

With the simplified assumptions of our calculations, only an agreement of the general structure of the theoretical level scheme with the experiment can be expected. The three β components shown might lead to three core-excited states of adjacent spin, the energies of which are shifted compared to the Pb²⁰⁸ states by interaction with the extra neutron pair. The 3.52-MeV state is likely to be a 5^- state decaying with nearly equal intensities to the 4^+ and 6^+ state of the $(2g_{9/2})^2$ configuration. The 2.40-MeV level decaying only to the 1.09-MeV 4^+ state should be 4^+ or 4^-, and might be identified with the 4^+ level of the $(1i_{11/2})^2$ configuration. The level group close to 2 MeV can be probably ascribed to the $(2g_{9/2}, 1i_{11/2})$ configuration.

The theoretical scheme served as guidance for placing the 83-keV transition above the 4^+ state of the ground-state configuration, although the quantitative agreement of energies is poorer than expected here. An extensive calculation of the Pb²¹⁰ levels with finite range forces and configuration mixing is in preparation.